Journal of Molecular Catalysis A: Chemical 388–389 (2014) 47–55

Contents lists available at ScienceDirect

Journal of Molecular Catalysis A: Chemical

journal homepage: www.elsevier.com/locate/molcata

Selective conversion of m-cresol to toluene over bimetallic Ni–Fe catalysts

Lei Nie, Priscilla M. de Souza[1,2], Fabio B. Noronha[1,2], Wei An[3], Tawan Sooknoi[4], Daniel E. Resasco*

School of Chemical, Biological, and Materials Engineering, The University of Oklahoma, Norman, OK 73019, USA

ARTICLE INFO

Article history:
Received 12 May 2013
Received in revised form
17 September 2013
Accepted 21 September 2013
Available online 12 October 2013

Keywords:
Ni–Fe/SiO_2
Hydrodeoxygenation
Cresol
Biomass
Tautomerization

ABSTRACT

The catalytic conversion of m-cresol in the presence of H_2 has been investigated on SiO_2-supported Ni, Fe, and bimetallic Ni–Fe catalysts at 300 °C and atmospheric pressure. Over the monometallic Ni catalyst, the dominant product is 3-methylcyclohexanone while 3-methylcyclohexanol and toluene appear in smaller amounts, even at high conversions. By contrast, on Fe and Ni–Fe bimetallic catalysts, the dominant product is toluene while the hydrogenation products (3-methylcyclohexanone and 3-methylcyclohexanol) are practically negligible in the entire range of conversions.

To explain these differences, we have proposed a deoxygenation path that starts with the tautomerization of m-cresol to an unstable ketone intermediate (3-methyl-3,5-cyclohexadienone). The fate of this intermediate is determined by the ability of the catalyst to either hydrogenate the carbonyl group or the ring. The former would mostly occur on Fe and Ni–Fe catalysts that contain an oxophilic metal (Fe), while the latter would occur on Ni, which has a higher affinity for the aromatic ring.

Hydrogenation of the carbonyl group produces a very reactive unsaturated alcohol (3-methyl-3,5-cyclohexadienol), which can be easily dehydrated to toluene. This would explain the high selectivity of Fe and Ni–Fe to toluene. By contrast, hydrogenation of the ring would result in 3-methylcyclohexanone, which can be further hydrogenated to 3-methylcyclohexanol. On supports that contain acid sites, which are active for dehydration, the formation of toluene would occur via dehydration of the alcohol and subsequent dehydrogenation. On the catalysts investigated in this work, dehydration of the corresponding alcohol does not occur, so the only path to toluene is via hydrogenation of the carbonyl of the unstable ketone intermediate.

In addition, to the products mentioned above, xylenol is also observed in significant yields, which indicate that transalkylation of m-cresol is another reaction path occurring on these catalysts.

1. Introduction

Phenolics are abundant components of the liquid product (bio-oil) obtained from the fast pyrolysis of biomass. They derive from both pyrolytic decomposition of lignin and condensation/aromatization of small oxygenates. They can represent an important building block for potential production of fuels and chemicals from biomass. However, following the primary conversion step, an effective catalytic upgrading step is needed in the production of useful products [1–6]. As we have previously pointed out [7], the upgrading process should not only minimize the oxygen content in the product, but also maximize carbon retention. As a result, conventional hydrotreating, the most common and effective method that has been tested for hydrodeoxygenation [8,9] may not be the optimum path for upgrading of bio-oil with maximum carbon efficiency. We have recently investigated different paths, including ketonization, aldol condensation, aromatization and alkylation to accomplish the formation of C—C bonds before deoxygenation, which maximizes the liquid fuel yield and carbon efficiency [10–12].

Several groups have investigated the use of sulfided catalysts (e.g., CoMo, NiMo) typically used in conventional hydrotreating for the deoxygenation of biomass-derived feedstocks [13]. These catalysts require addition of H_2S to remain stable and active; however, sulfidation is not required in the HDO of biomass-derived

* Corresponding author. Tel.: +1 405 325 4370; fax: +1 405 325 5813.
E-mail address: resasco@ou.edu (D.E. Resasco).
[1] Permanent address: Depto de Engenharia Química/Instituto Militar de Engenharia, Praça Gal. Tiburcio, 80, CEP 22290-270, Rio de Janeiro, Brazil.
[2] Permanent address: Instituto Nacional de Tecnologia (INT), Laboratório de Catálise, sala 518, Av. Venezuela 82, CEP 20081-312, Rio de Janeiro, Brazil.
[3] Permanent address: Chemistry Department, Brookhaven National Laboratory, P.O. Box 5000, Upton, NY 11973-5000, USA.
[4] Permanent address: King Mongkut's Institute of Technology Ladkrabang, Chalongkrung Road, Ladkrabang, Bangkok 10520, Thailand.

1381-1169/$ – see front matter © 2013 Elsevier B.V. All rights reserved.
http://dx.doi.org/10.1016/j.molcata.2013.09.029

feedstocks since hydrodesulfurization is not a necessary requirement. Thus, noble metal catalysts (e.g., Pt, Pd) can become attractive since they are significantly more active for HDO than other catalysts. For example, bifunctional Pt/Al_2O_3 [14,15] and Pt/H-beta zeolite [16] have been found to be active for the deoxygenation of oxygenated aromatics. However, the high cost of noble metals may be an impediment for practical applications. The search for alternative catalysts based on non-noble metals (e.g., Ni, Fe, Co, Ga) has been the focus of several recent studies [17–22]. The combination of metal sites (active for hydrogenation) with acid sites provided by the support or added promoters (active for transalkylation and dehydration) can optimize the catalyst resulting in improved deoxygenation activity and carbon efficiency.

The use of bimetallic catalysts adds another interesting aspect since changes in electronic structure and/or surface ensemble size due to the presence of adjacent atoms may greatly modify the resulting selectivity [17,19]. In recent studies, Ni and Ni–Cu catalysts have been evaluated for the HDO of guaiacol [23–25]. The studies agree that the addition of Cu improves the catalyst performance for HDO. Similarly, in a recent investigation of our own group, Ni–Fe bimetallic catalysts were evaluated for the hydrogenation and deoxygenation of furfural as a model compound of sugar dehydration products. We found that the reaction pathways on Ni–Fe bimetallics were dramatically different from those on pure Ni or pure Fe catalysts. While pure Fe was inactive at the reaction conditions investigated, it greatly altered the behavior of Ni when added in 1:1 molar ratio. The high decarbonylation activity typically observed on pure Ni was suppressed on the bimetallic catalyst, while the C=O hydrogenation (at low temperatures) and C—O hydrogenolysis (at high temperatures) were drastically enhanced [26].

A mechanism for the deoxygenation of phenolic compounds that has been widely proposed in the literature [9,14,15,27] is the two-step pathway, which involves an initial hydrogenation of the aromatic ring followed by $C(sp^3)$—O bond cleavage via dehydration. This HDO pathway normally requires a bi-functional catalyst, with a metal function that catalyzes hydrogenation/dehydrogenation of the ring and an acid function that catalyzes dehydration. An alternative mechanism that has been suggested in several studies [27,28] does not involve the $C(sp^2)$-to-$C(sp^3)$ conversion. In analogy to the direct desulfurization (DDS) path typically proposed in HDS catalysts, a direct cleavage of the $C(sp^2)$—O bond has been claimed in several reports and referred to as direct deoxygenation (DDO) [27]. Since such cleavage would require a very high activation energy, one may expect that this path might only be possible at high temperatures.

In the present contribution, we investigate the different product distributions from the hydrodeoxygenation of m-cresol over Ni and Ni–Fe catalyst. While the three cresol isomers only represent a small fraction in the composition of a real bio-oil, they are present in significant amounts in the product of primary upgrading processes, such as catalytic pyrolysis or conversion of pyrolysis vapors preceding condensation, after which a final dehydroxygenation step is necessary. Nevertheless, we must emphasize that the main objective of the present contribution is to expand the fundamental understanding of the interactions of the hydroxyl group in phenolics with a bimetallic catalyst such as Ni–Fe in which one of the metals exhibit a high oxophilicity and may not be completely reduced under reaction conditions. The present study has allowed us to infer a novel reaction pathway that includes some important conceptual differences from those previously proposed in the literature.

2. Experimental

2.1. Catalyst synthesis and characterization

Monometallic catalysts Ni/SiO_2 and Fe/SiO_2 (5 wt% metal loading) were prepared by incipient wetness impregnation of the support (SiO_2, HiSil 233) with an aqueous solution of the respective metal precursor: $Ni(NO_3)_2{\cdot}6H_2O$ (98%, Alfa Aesar) and $Fe(NO_3)_3{\cdot}9H_2O$ (98% Sigma–Aldrich). As described in our previous work [26], the bimetallic $Ni–Fe/SiO_2$ catalysts were prepared by incipient wetness co-impregnation. In this case, the Ni loading was kept constant at 5.0 wt.% on all samples, while the Fe loading was varied from 2.0, 5.0 to 10 wt.%. As summarized in Table 1, they are indicated with the approximate mass ratios as (2:1)Ni–Fe, (1:1)Ni–Fe, and (1:2)$Ni–Fe/SiO_2$, respectively.

XRD analysis was conducted on samples pre-reduced ex situ under pure H_2 (100 ml/min) at 450 °C for 1 h and passivated by slow exposure to low O_2 concentrations at room temperature, before exposure to the atmosphere. The measurements were carried out with a D8 Series II X-Ray Diffractometer (BRUKER AXS) operated at 40 kV and 35 mA, using Cu Kα monochromatic radiation (λ = 0.154178 nm) in the 30–60° diffraction angle range.

The reducibility of the calcined samples was determined by temperature programmed reduction (TPR). In these measurements, 20 mg of a sample was placed in a quartz reactor and heated at 30 °C/min up to 500 °C under a He flow of 20 ml/min, and held at this temperature for 1 h. The reactor was then cooled down to 30 °C and the sample exposed to a stream of 5% H_2/Ar at a flow rate of 20 ml/min. Subsequently, the sample was heated to 800 °C at a heating rate of 5 °C/min. The variation in hydrogen uptake was monitored on a TCD detector as a function of temperature. The molar H_2 uptake per gram of sample was quantified from the peak area in the TPR profiles and calibrated with a CuO standard. Morphology and size of the Ni–Fe clusters were characterized by transmission electron microscopy (TEM, JEOL model JEM-2100 LaB6). Before TEM analysis, the samples were reduced ex situ in pure H_2 (100 ml/min) at 450 °C for 1 h. The reduced samples were then mixed with 2-propanol, sonicated, deposited onto the TEM (Cu) grids, and dried. Average particle sizes for all the samples, as determined by TEM, are summarized in Table 1. The BET surface area (Sg) was measured by conventional N_2 physisorption on a Micromeritics ASAP 2010 unit, after evacuation at 350 °C for 3 h.

The surface chemistry of the catalysts was investigated by Diffuse Reflectance Infrared Fourier Transform Spectroscopy (DRIFTS) of adsorbed pyridine. For these measurements, the catalyst powder was loaded in the sample cup, reduced in situ at 400 °C for 1 h under a flow of H_2 (30 ml/min) and cooled down to 100 °C. Then, pyri-

Table 1
Characterization of catalysts from Ref. [26].

Catalysts	Wt%Ni	Wt%Fe	BET (m^2/g)	H_2 comsumption from TPR (mmol/gcat)	Diameter (nm)	Lattice constant (Å)		
						XRD	DFT	Std.
Ni	5	0	126	1.01	11.2	3.53	3.52	3.52
(2:1)Ni–Fe	5	2	130	1.48	10.0	3.57	–	–
(1:1)Ni–Fe	5	5	115	2.20	10.0	3.58	3.55[a]	3.58[a]
(1:2)Ni–Fe	5	10	124	–	9.6	3.58	–	–
Fe	0	5	128	–	19.1	2.87	–	2.87

dine vapor was passed through the cell for approximately 30 min. To eliminate the weakly bound pyridine, the sample was purged under H_2 flow for 20 min at 100 °C. Background and absorption spectra were recorded at a resolution of 4 cm^{-1}, accumulating 256 scans.

2.2. Catalytic activity measurements

The vapor-phase conversion of m-cresol in H_2 over the Ni, Ni–Fe and Fe catalysts was evaluated in a tubular quartz reactor at atmospheric pressure. The flow reaction system is equipped with a mass flow controller and a syringe pump for the continuous injection of m-cresol. All lines were heated to avoid condensation of the compounds. Pelletized catalyst (40–60 mesh) was packed in the reactor between two layers of quartz wool and a preheating layer of glass beads on top to improve the temperature uniformity. The catalyst was reduced in situ under a down-flow of 60 ml/min of H_2 at 450 °C for 1 h, and then the temperature was reduced to the reaction temperature 300 °C. The H_2/m-cresol molar ratio was kept at 60:1 for all runs. The products were quantified by gas chromatography (GC 6890, Agilent), using an Innowax capillary column and a flame ionized detector (FID). The catalyst was evaluated under different W/F (0.058–0.464 h) varying the amount of catalyst (30–120 mg). The W/F is defined as the ratio of the catalyst mass (g) to organic feed flow rate (g/h). The product yield and selectivity for each product were calculated as follows:

$$\text{Yield}\,(\%) = \frac{\text{mol of product}}{\text{mol of m-cresol fed}} \times 100$$

$$\text{Selectivity}\,(\%) = \frac{\text{mol of product}}{\text{mol of m-cresol consumed}}$$

2.3. Computational method

DFT calculations were performed in the Vienna ab initio simulation package (VASP) [29,30]. A spin-polarized GGA PBE functional [31], all-electron plane-wave basis sets with an energy cutoff of 400 eV, and a projector augmented wave (PAW) method [32,33] were adopted. The Ni(1 1 1), Fe(1 1 0) and NiFe(1 1 1) surfaces were modeled by a three-layer p(4 × 4) slab with the bottom two layers fixed at their optimized bulk positions. The calculated lattice constants are 3.522 Å for fcc Ni, 2.831 Å for bcc Fe, and $a = c = 3.553$ Å $b = 3.582$ Å for fcc Ni_2Fe_2. The two successive slabs were separated by a 18 Å vacuum region. Considering that the surface composition may differ from that of the bulk alloy and surface segregation may occur in a NiFe alloy [34], we also considered a model that contains "disordered" NiFe alloy surface, which has the same Ni:Fe molar ratio of 1:1 as the perfect surface, but is re-arranged to create "islands" of Ni and Fe. Such a "disordered" surface is energetically unfavorable compared to the perfect one, i.e., having energy penalty of 0.39 kcal/mol per surface atom. The previous Mössbauer investigation [35] suggested that certain phase separation could accompany particle growth in NiFe alloy catalysts using the similar synthesis process as in this work. The 3 × 3 × 1 *k*-points using the Monkhorst–Pack scheme was used in the calculations. First-order Methfessel–Paxton smearing of 0.2 eV was employed in the integration to speed up the convergence. The conjugate gradient algorithm was used in the optimization. The convergence threshold was set 10^{-4} eV in total energy and 10^{-2} eV/Å in force on each atom. The adsorption energy (Eads) is defined as Eads = *E*(cresol/slab) – Eslab – *E*(cresol), where *E*(cresol/slab), Eslab, and *E*(cresol) are the total energy of cresol/slab, clean surface, and gas-phase m-cresol in one supercell, respectively.

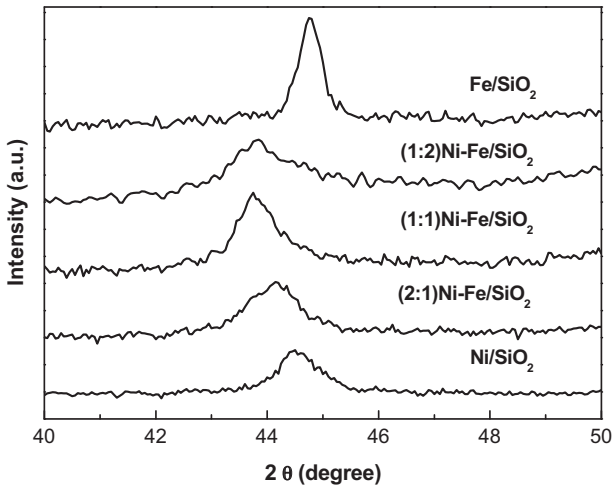

Fig. 1. XRD patterns of monometallic Ni, Fe and bimetallic Ni–Fe catalysts pre-reduced ex situ in hydrogen at 450 °C for 1 h.

3. Results and discussion

3.1. Catalyst characterization

Fig. 1 displays the XRD patterns of the catalyst samples after H_2 reduction. The monometallic Ni catalyst showed one peak at $2\theta = 44.41°$, which is ascribed to the Ni(1 1 1) reflection. The bimetallic catalysts exhibited a single peak around this region, but shifted to lower angles with increasing Fe content. In agreement with previous studies [19,26,36], these XRD data indicate the formation of a Ni–Fe solid solution, rich in Ni. The shift to lower angles with Fe content indicates an increase in the Fe concentration in the solid solution. In addition to the peak corresponding to the Ni–Fe solid solution, the sample with the highest Fe concentration (1:2)Ni–Fe/SiO_2, exhibited a shoulder at $2\theta = 44.64°$, which is ascribed to the α-Fe(1 1 0) reflection resulting from a fraction of unalloyed Fe. The same result has been observed in previous XRD studies conducted on a sample of Fe/Ni = 2 ratio, and the authors assigned this double peak to unalloyed α-Fe or Fe-rich alloys with a bcc structure [36]. The TPR profiles [26] also support the formation of bimetallic clusters in the Fe–Ni catalysts. The characterization results of the catalysts are summarized in Table 1; further details about these catalysts can be found in our previous publication [26].

DRIFTS of adsorbed pyridine was conducted on the different catalysts to compare their surface properties. The DRIFT spectra obtained on the Ni, (1:2)Ni–Fe, and Fe/SiO_2 catalysts after exposure to pyridine at atmospheric pressure and 100 °C are reported in Fig. 2, along with the spectrum obtained on pure SiO_2 exposed to pyridine. An intense band at 3741 cm^{-1} (not shown) corresponding to the silanol O—H stretching mode was observed for all samples [37]. No absorption band was observed for the SiO_2 support in the frequency region corresponding to adsorbed pyridine (1620–1420 cm^{-1}). Therefore, it can be concluded that any contribution to the spectra of pyridine interacting with hydrogen-bonded or free silanol [38] are negligible under the conditions of the measurements (i.e., purged at 100 °C). By contrast, the catalysts do display pronounced absorption bands at 1445, 1577 and 1596 cm^{-1}, which are characteristic of the vibrational modes 19b and 8a of pyridine species interacting with coordinatively unsaturated cations [39,40]. According to the relative band intensity for comparable amounts of catalyst and surface areas, we can estimate that the density of coordinatively unsaturated cations increases in the order Ni/SiO_2 < (1:2)Ni–Fe/SiO_2 < Fe/SiO_2. The presence of

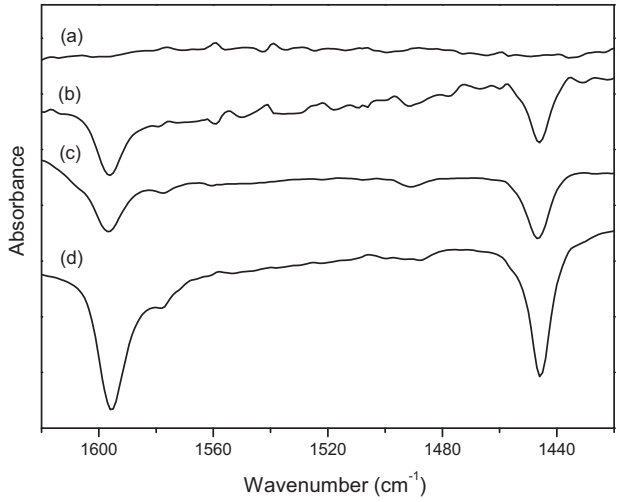

Fig. 2. DRIFT spectra of the pyridine chemisorption experiments at 100 °C and atmospheric pressure after pyridine chemisorptions for (a) pure SiO_2, (b) Ni/SiO_2, (c) (1:2)Ni–Fe/SiO_2, (d) Fe/SiO_2.

unreduced cations remaining on the surface of silica even after high temperature reduction treatments has been demonstrated for Fe/SiO_2 [40] as well as for Ni/SiO_2 [41].

3.2. Catalytic activity and product distribution at varying m-cresol conversion

The product distribution from the m-cresol conversion over Ni/SiO_2 at 300 °C is shown in Fig. 3 as a function of W/F. Three C_7 compounds are obtained, 3-methylcyclohexan (ONE) that is the main product, 3-methylcyclohexan (OL), and toluene (TOL). In addition to the three C_7 compounds, methane, phenol, and xylenol are also obtained as products. They may arise from hydrogenolysis and transalkylation side reactions. Metallic Ni is a well-known hydrogenolysis catalyst, but transalkylation (disproportionation) is typically catalyzed by acid sites. While the silica support provides no significant acidity, a fraction of Ni may not be fully reduced, as described above. The presence of coordinatively unsaturated cations may act as Lewis acid sites [40], which might catalyze the transalkylation that produces phenol and xylenol. On the other hand, methane may arise from metal-catalyzed hydrogenolysis or acid-catalyzed demethylation.

A remarkable difference in product distribution relative to that obtained on Ni/SiO_2 is observed on the iron-containing Fe and Ni–Fe/SiO_2 catalysts when compared under identical reaction conditions. As summarized in Table 2, when the three different catalysts are compared at 300 °C and W/F = 0.46 h a drastic change in product selectivity is observed. While, as mentioned above, 3-methylcyclohexanone is the dominant C_7 compound over Ni/SiO_2 it is not formed either on Fe or Ni–Fe/SiO_2 catalysts. By contrast, on these catalyst the largely dominant product is toluene (TOL). Interestingly, the physical mixture of Fe/SiO_2 and Ni/SiO_2 catalysts behaves very similarly to the Ni/SiO_2 catalyst alone. That is, ring hydrogenation products were formed and 3-methylcyclohexanone was the main one. Small amounts of toluene and xylenol were observed on this mixture, while they were the main products over the bimetallic catalysts, which may be due to the rather low activity of Fe/SiO_2 compared to Ni/SiO_2. Thus, these results demonstrate that the typical behavior of unalloyed Ni is not observed on the Ni–Fe bimetallic surface. As discussed below, the observed difference in behavior may be due to surface enrichment of Fe, or at least, the formation of Fe islands on the surface, as suggested by the DFT results discussed in section 3.4 below.

The Fe-containing catalysts also produce xylenols, xylene, phenol, and methane. In this case, again, the transalkylation reaction responsible for the production of C8 products might be catalyzed by the Lewis acid sites created by the presence of coordinatively unsaturated cations of unreduced Fe and/or Ni.

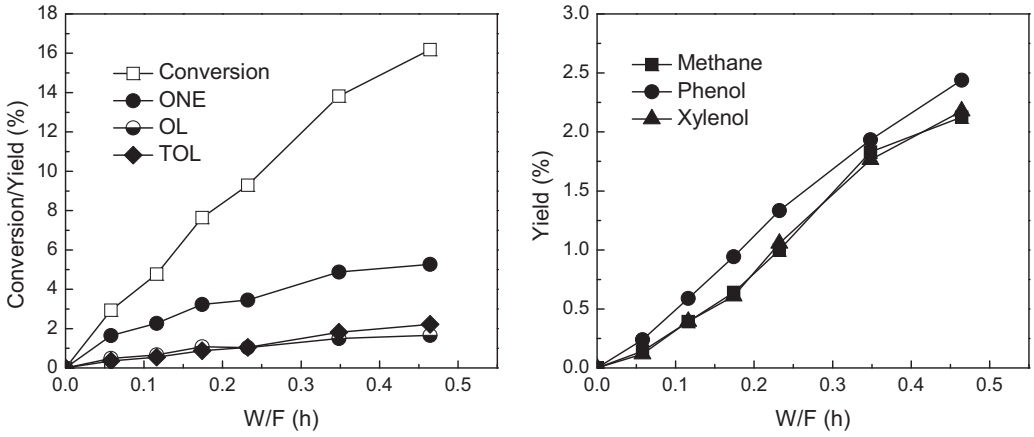

Fig. 3. Product distribution of m-cresol over 5% Ni/SiO_2 at 300 °C as a function of W/F H_2/feed molar ratio = 60. Pressure = 1 atm.

Table 2
Conversion and product selectivity from the reaction of m-cresol over different catalysts at W/F = 0.46 h and 300 °C. H_2/feed molar ratio = 60. Pressure = 1 atm.

	5% Ni/SiO_2	5% Fe/SiO_2	5% Ni/SiO_2 + 5% Fe/SiO_2 (physical mixture)	5% Ni–5% Fe/SiO_2
Conversion %	16.2	8.8	12.6	13.7
Selectivity %				
Toluene	14.2	60.2	18.5	52.6
3-Methylcyclohexanone	33.3	0.0	33.1	0.0
3-Methylcyclohexanol	11.1	0.0	13.7	0.0
Methane	13.0	0.0	10.5	2.2
Transalkylation Products	28.4	39.8	24.2	45.3

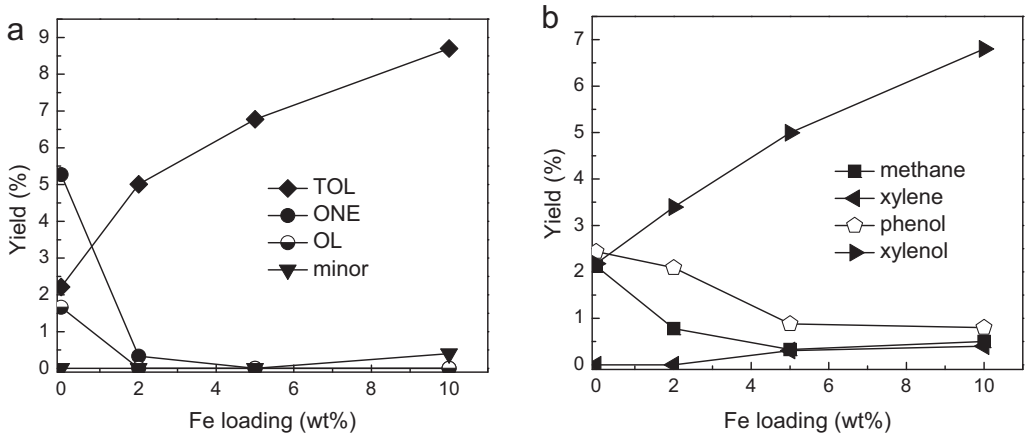

Fig. 4. Yield of products of m-cresol over Ni–Fe bimetallic catalysts as a function of Fe loading at 300 °C. H_2/feed ration = 60. Pressure = 1 atm. W/F = 0.46 h. (a) C7 products: 3-methyl-cyclohexanone (ONE); 3-methylcyclohexanol (OL); toluene (TOL); (b) transalkylation and hydrogenolysis products.

Fig. 4 shows the effect of Fe in the catalyst on the product distributions obtained at 300 °C at a fixed W/F (0.46 h). It is interesting to note that the yield of toluene increases with increasing Fe loading. This clearly shows that the addition of Fe improves the deoxygenation activity. However, the pure Fe catalyst exhibits a lower yield to toluene, i.e., about 5% for the same conditions (see Table 2). The second interesting trend is that the yields of 3-methylcyclohexanone and 3-methylcyclohexanol decrease with increasing Fe loading. Only a small fraction of 3-methylcyclohexanone is observed over (2.5:1)Ni–Fe/SiO_2, but essentially zero on the other catalysts. This result indicates that the addition of Fe inhibited the hydrogenation of the ring.

Finally, as shown in Fig. 4b, the yields of xylenol (transalkylation product) increase appreciably with increasing Fe loading. This may be related to the increasing amount of Lewis acidity created by unreduced Fe, as discussed in Fig. 2. In line with these findings, a recent study [23] on Ni and Ni–Cu catalysts used for the HDO of guaiacol indicated that the selectivity for methyl-substitution compounds increased with addition of Cu due to improvement of the acidic properties on the catalyst surface.

Fig. 5 shows the product distributions for m-cresol conversion on the (1:2)Ni–Fe/SiO_2 as a function of W/F. The yields of toluene and xylenol are the two major products and their yields increase with W/F. By contrast, the hydrogenation products 3-methylcyclohexanone and 3-methylcyclohexanol are negligible at all W/F.

Fig. 6 shows the product selectivities as a function of m-cresol conversion. Over Ni/SiO_2, the selectivity to 3-methylcyclohexanone is the highest, around 60%, while the selectivities to 3-methylcyclohexanol and toluene are both around 20%. Over (1:2)Ni–Fe/SiO_2, toluene is the only dominant one, whose selectivity is almost 100% along all conversion. This again shows that addition of Fe to Ni/SiO_2 helps enhance the deoxygenation activity dramatically. The variation of activity with time on stream over the Ni and Ni–Fe/SiO_2 catalysts is compared in Fig. 7. While both of them show some deactivation as a function of time, the bimetallic catalyst seems to be slightly more stable.

3.3. Using 3-methylcyclohexanone and 3-methylcyclohexanol as feeds

Table 3 compares the product distributions obtained by feeding 3-methylcyclohexanol (OL), 3-methylcyclohexanone (ONE), or m-cresol over the monometallic and bimetallic catalysts. When 3-methylcyclohexanol was fed over the Ni/SiO_2 catalyst, it was quickly converted to 3-methylcyclohexanone. Similarly, when 3-methylcyclohexanone was the feed, the corresponding alcohol was obtained at high yield. These results indicate that this is a fast and reversible reaction. In both cases, m-cresol was also observed as a product, but toluene was not obtained. To get the same level of conversion with m-cresol the W/F had to be raised by almost 20 times since the rate of interconversion between 3-methylcyclohexanol

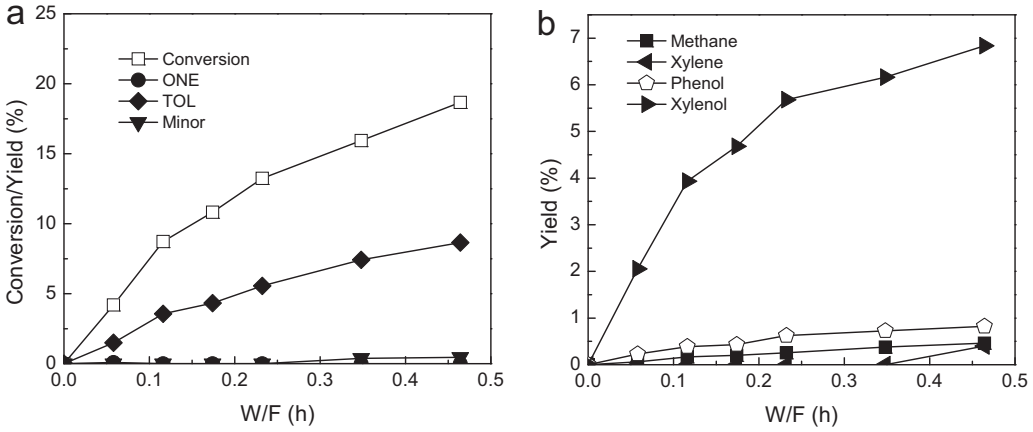

Fig. 5. Product distribution of m-cresol over (1:2)Ni–Fe/SiO2 at 300 °C as a function of W/F. H_2/feed ration = 60. Pressure = 1 atm. (a) C7 products: 3-methylcyclohexanone (ONE); 3-methylcyclohexanol (OL); toluene (TOL); (b) transalkylation and hydrogenolysis products.

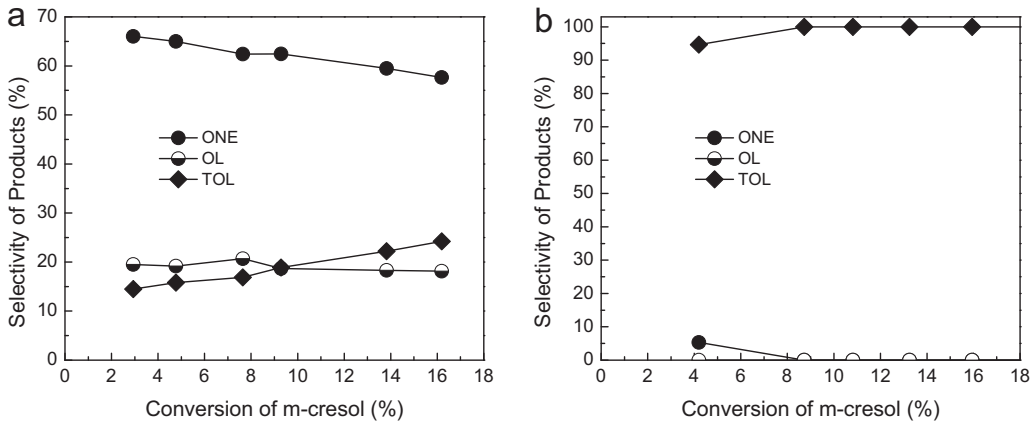

Fig. 6. C7 Product selectivity as a function of conversion of m-cresol at 300 °C. a. Ni/SiO_2; b. (1:2)Ni–Fe/SiO_2. H_2/feed molar ratio = 60. Pressure = 1 atm. C7 products: 3-methylcyclohexanone (ONE); 3-methylcyclohexanol (OL); toluene (TOL).

Table 3
Product distribution from different feed at 300 °C. H_2/feed molar ratio = 60. Pressure = 1 atm. C_7 products: 3-methyl-cyclohexanone (ONE); 3-methylcyclohexanol (OL); toluene (TOL); methylcyclohexane (ENE).

Catalyst	Feed	OL	ONE	m-Cresol
Ni/SiO_2	W/F (h)	0.02	0.02	0.36
	Conversion (%)	13.8	16.6	13.8
	Yield (%)			
	ONE	11.5	–	4.9
	OL	–	8.3	1.5
	m-Cresol	2.3	8.3	–
	TOL	0	0	1.8
	ENE	0	0	0
	Transalkylation	0	0	5.6
(1:2)Ni–Fe/SiO_2	W/F (h)	0.02	0.02	0.12
	Conversion (%)	8.7	7.6	8.7
	Yield (%)			
	ONE	8.2	–	0
	OL	–	7.1	0
	m-Cresol	0.3	0.3	–
	TOL	0	0	3.6
	ENE	0.5	0.2	0
	Transalkylation	0	0	5.1
SiO_2	W/F	0.46		
	Conversion (%)	0.3		

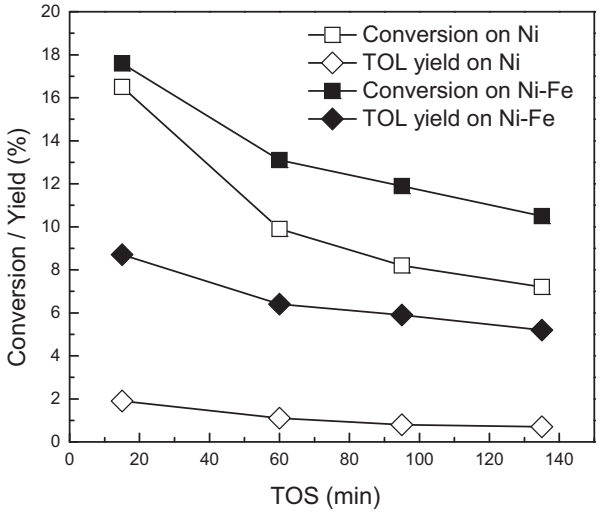

Fig. 7. Effect of time on stream on of conversion of m-cresol and toluene yield over Ni/SiO_2. (open symbol) and (1:2)Ni–Fe/SiO_2 (solid symbol) at 300 °C. H_2/feed ration = 60. Pressure = 1 atm. Toluene (TOL).

and 3-methylcyclohexanone is much faster than the conversion of m-cresol to either of these compounds, which would suggest that during the HDO of m-cresol the saturated alcohol and ketone are pseudo-equilibrated.

Interestingly, the absence of toluene as a product when 3-methylcyclohexanol was the feed indicates that dehydration does not occur to any significant extent at the low W/F used (i.e., 0.02 h). To further investigate the role of dehydration on the support, 3-methylcyclohexanol was fed at the same W/F as used with m-cresol (i.e., W/F = 0.36 h) over pure SiO_2. As shown in Table 3, no conversion was observed.

In addition, a significant fraction of the products from m-cresol over Ni/SiO_2 are due to transalkylation (xylenols, xylene, phenol). However, this reaction did not occur when 3-methylcyclohexanol or 3-methylcyclohexanone was used as a feed at W/F = 0.02 h.

One of the most interesting differences observed over the bimetallic Ni–Fe/SiO_2 catalyst was the appearance of the alcohol dehydration product methylcyclohexene (ENE). This product was particularly abundant when 3-methylcyclohexanol was used as feed. The Lewis acid sites present on the bimetallic catalyst might be responsible for the observed dehydration. However, even in this case, no toluene was formed. This further proves that the dehydration of 3-methylcyclohexanol cannot give toluene under this

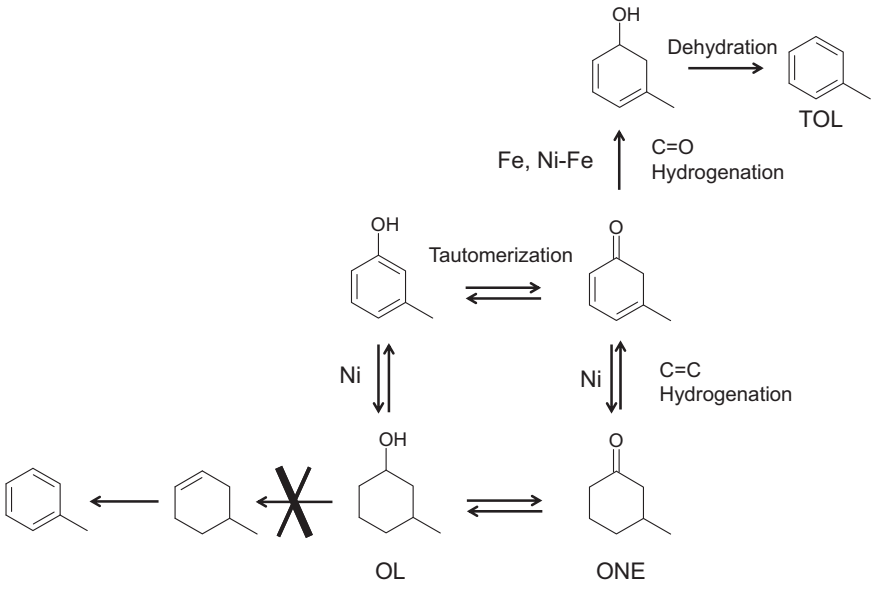

Scheme 1. HDO reaction pathways over Ni, Fe, and Ni–Fe catalysts.

reaction conditions. Again, 3-methylcyclohexanone and m-cresol were seen as products from 3-methylcyclohexanol.

When feeding 3-methylcyclohexanone over the bimetallic catalyst, the hydrogenation product 3-methylcyclohexanol and dehydrogenation product m-cresol are detected. As in the previous case, methylcyclohexene is also formed from the dehydration of methylcyclohexanol, but no toluene is detected. An interesting question arises when comparing these trends. If m-cresol is readily formed when feeding either 3-methylcyclohexanol or 3-methylcyclohexanone, why is toluene not formed by ring dehydrogenation from methylcyclohexene? If m-cresol were produced by ring dehydrogenation of 3-methylcyclohexanol the dehydrogenation of methylcyclohexene to toluene would be much easier. As discussed below, the reason for this discrepancy is that m-cresol is not directly produced from 3-methylcyclohexanol, but rather from 3-methylcyclohexanone.

3.4. Mechanistic implications of the observed product distributions

The significant differences observed between the m-cresol conversion over Ni or over Fe-containing catalysts may be explained in terms of a reaction pathway that we summarize in Scheme 1, which can account for all the results and product trends reported above.

First, we propose that over Ni/SiO_2 at least two parallel pathways may exist. One is the direct hydrogenation of the aromatic ring to 3-methylcyclohexanol, which could be dehydrated and then dehydrogenated to toluene. However, a second (indirect) path can also exist and this might be crucial for the highly selective production of toluene. It is known that m-cresol can tautomerize to a highly unstable methyl cyclohexadienone. While this intermediate cannot be detected under reaction conditions, we may anticipate that depending on the catalyst, it could result in:

(a) methyl cyclohexanone, when the double bonds in the ring are hydrogenated, or
(b) methyl cyclohexadienol, when the C=O group is hydrogenated.

The preference in hydrogenating the ring or the carbonyl group strongly depends on the catalyst used. For example, Group VIII metal catalysts such as Ni, Pt, or Pd have a strong affinity for the aromatic ring and/or C=C. On these metals aromatics and/or olefins adsorb parallel to the surface and they are highly active for ring and/or C=C saturation [42–47]. When Group VIII metals are alloyed with oxophilic metals such as Sn, Re, or Fe we may anticipate that the interaction with the ring will be decreased while the interaction with the carbonyl group will be enhanced. This is in fact the case for α,β-unsaturated aldehydes, for which Group VIII metals result in saturation of the C=C double bond, but bimetallics such as Pt–Sn or Pt–Fe that contain oxophilic elements produce unsaturated alcohols [48–52].

We may expect that this chemoselective hydrogenation of the carbonyl group may occur in our case for the conversion of m-cresol over Fe-containing catalysts.

Therefore, in case (a), which is typical of Ni, 3-methylcyclohexanone becomes dominant (Table 3). This product can be further hydrogenated to 3-methylcyclohexanol. As mentioned above, if the support contains enough acidity to catalyze the dehydration of the saturated alcohol 3-methylcyclohexanol, toluene could be obtained after dehydration/dehydrogenation, as previously proposed for the conversion of phenol over Ni/SiO_2 [53] and cresol over Pt catalysts [22]. As reported previously [9,14,22], over a bi-functional catalyst containing acid and metal functions, the deoxygenation of phenolic compounds proceeds via hydrogenation of the aromatic ring to the corresponding alcohols followed by dehydration to the olefin then dehydrogenated back to aromatic. However, over our Ni/SiO_2 catalyst under the reaction conditions investigated, dehydration does not occur to a significant extent. As shown in Table 3, when we fed 3-methylcyclohexanol over Ni/SiO_2, we did not observe any formation of toluene or methylcyclohexene. Only dehydrogenation of 3-methylcyclohexanol to 3-methylcyclohexanone and cresol was seen. This indicates that toluene does not derive from the dehydration/dehydrogenation of the 3-methylcyclohexanol.

In case (b), since hydrogenation of the aromatic ring is suppressed on the Fe-containing catalysts, the deoxygenation of m-cresol requires the participation of its keto tautomer methylcyclohexadienone intermediate. Once the carbonyl group of such species is hydrogenated, the resulting methylcyclohexadienol can be readily dehydrated to toluene, which is driven by aromatic stabilization. The electrophilic character of unreduced metal (either Fe or Ni) might help stabilize the tautomer intermediate, thus enhancing the deoxygenation activity [54]. Due to its oxophilicity, Fe is

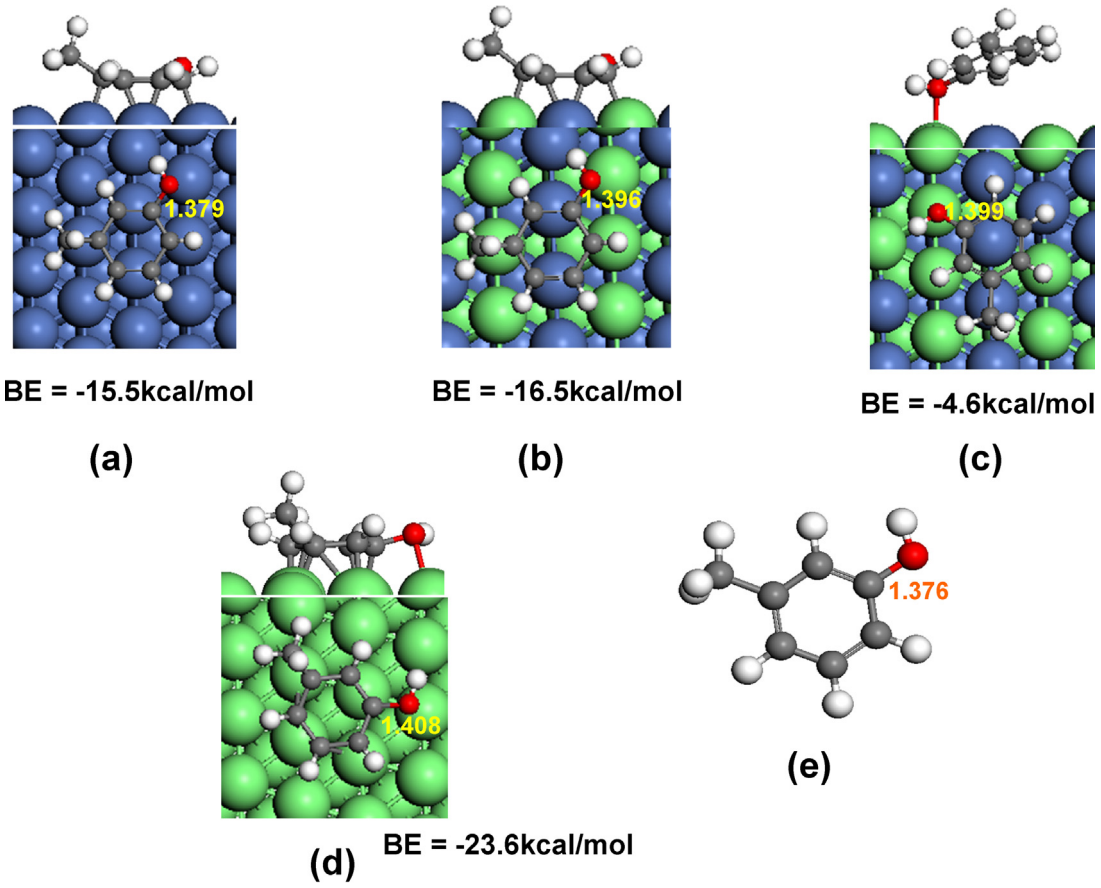

Fig. 8. Optimized adsorption structures of m-cresol on (a) Ni(1 1 1) surface, (b) perfect NiFe(1 1 1) surface, (c) patched NiFe(1 1 1) surface and (d) Fe(1 1 0) surface. (e) Gas phase. C—OH bond lengths are labeled in each molecule.

more efficient in linking to the O of the carbonyl than Ni, which in turn has a higher affinity for the aromatic ring. Hence, case (b) is largely promoted over Fe containing catalysts resulting in enhanced deoxygenation activity. It must be emphasized that although the products from this pathway would appear to result from a direct C(sp^2)—O cleavage, i.e., DDO, this is not the case. This is a pathway that requires a relatively low activation energy and is more likely to occur under the reaction conditions investigated (300 °C, atmospheric H_2).

As reported in our previous study on furfural and benzaldehyde [26], the addition of Fe to the monometallic Ni catalyst, suppresses hydrogenation of the ring. The reason for this activity drop may be that Fe causes repulsion to the π electron system of the ring. As shown in the DFT calculations below, this repulsion is particularly pronounced when the Ni–Fe particles show a non-uniform distribution, forming Fe patches on the surface. Thus, it is then expected that Ni–Fe and Fe catalysts will have a poor aromatic ring hydrogenation activity compared to Ni catalysts [3,18,55]. By contrast, the presence of Fe promotes the hydrogenation of the C=O group.

3.5. DFT calculation

We have calculated the energetics of the adsorption of m-cresol on Ni(1 1 1), Fe(1 1 0) and NiFe(1 1 1) alloy surface, which can provide information on how m-cresol molecules interact with the metal surfaces. As shown in Fig. 8, the m-cresol prefers a flat adsorption configuration on Ni(1 1 1) Fe(1 1 0) and bulk-terminated NiFe(1 1 1) alloy surface, but a slanted configuration on a patchy NiFe(1 1 1) alloy surface due to repulsion of the phenyl ring. The reason for the major difference is in line what was proposed above from the analysis of the reaction products. That is, the interaction with the O of the C—O is strongest on the Fe(1 1 0) surface, followed by the NiFe(1 1 1) alloy and negligible or rather repulsive on the Ni(1 1 1) surface. If the C—O bond elongation is used as an indicator for the M—O affinity a clear trend is observed, i.e., 1.408 Å > 1.399 (1.396) > 1.379 > 1.376 for the Fe, Ni–Fe, Ni, and gas-phase, respectively.

Note that the calculated binding energy of m-cresol on Fe(1 1 0) (−23.6 kcal/mol) is even higher than that on Ni(1 1 1) (−15.5 kcal/mol) or the bulk-terminated alloy NiFe(1 1 1) (−16.5 kcal/mol). However, in the case of Fe(1 1 0) the enhanced adsorption energy is due to a strong interaction with the oxygenated group rather than the ring.

4. Conclusion

A novel type of catalyst has been identified that shows high selectivity for hydrodeoxygenation of phenolic compounds. It is demonstrated that when the catalyst contains an oxophilic metal, such as Fe, the chemoselective hydrogenation of a keto tautomer intermediate can be greatly enhanced, resulting in a cyclodiene alcohol that is readily dehydrated to the aromatic hydrocarbon, favored by the stabilization provided by the aromaticity of the product. This mechanism does not involve the partial hydrogenation of the ring nor a direct C(sp^2)—O cleavage, as has been previously proposed. By contrast, when Fe is not present, the Ni-containing catalyst preferentially interacts with the aromatic ring and promotes its saturation, producing 3-methyl-cyclohexanone and 3-methylcyclohexanol. On the catalysts investigated here, these saturated rings are not able to produce toluene via dehydration/

dehydrogenation. In addition to these C_7 products, some transalkylation products are also observed. It is proposed that they arise from Lewis acids associated with the incomplete reduction of Fe and/or Ni cations.

Acknowledgments

Support from the National Science Foundation (NSF EPSCoR 0814361) and the Department of Energy (DE-FG36GO88064) is greatly appreciated. Allocation of computing time provided by the OU Supercomputing Center for Education and Research (OSCER) at the University of Oklahoma is acknowledged. We thank CAPES, Brazil for a scholarship for one of us (PMS).

References

[1] P.M. Mortensen, J.-D. Grunwaldt, P.A. Jensen, K.G. Knudsen, A.D. Jensen, Appl. Catal. A: Gen. 407 (2011) 1–19.
[2] G.W. Huber, S. Iborra, A. Corma, Chem. Rev. 106 (2006) 4044–4098.
[3] R. Olcese, M.M. Bettahar, B. Malaman, J. Ghanbaja, L. Tibavizco, D. Petitjean, A. Dufour, Appl. Catal. B 129 (2013) 528–538.
[4] D.M. Alonso, S.G. Wettstein, J.A. Dumesic, Chem. Soc. Rev. 41 (2012) 8075–8098.
[5] P.M. Mortensen, J.D. Grunwaldt, P.A. Jensen, K.G. Knudsen, A.D. Jensen, Appl. Catal. B 407 (2011) 1–19.
[6] S. Echeandia, P.L. Arias, V.L. Barrio, B. Pawelec, J.L.G. Fierro, Appl. Catal. B 101 (2010) 1–12.
[7] D.E. Resasco, J. Phys. Chem. Lett. 2 (2011) 2294–2295.
[8] A. Ausavasukhi, Y. Huang, A.T. To, T. Sooknoi, D.E. Resasco, J. Catal. 290 (2012) 90–100.
[9] E. Furimsky, Appl. Catal. A 199 (2000) 147–190.
[10] P.A. Zapata, J. Faria, M.P. Ruiz, D.E. Resasco, Top. Catal. 55 (2012) 38–52.
[11] L. Nie, D.E. Resasco, Appl. Catal. A 447–448 (2012) 14–21.
[12] T.N. Pham, D. Shi, T. Sooknoi, D.E. Resasco, J. Catal. 295 (2012) 169–178.
[13] D.C. Elliott, Energy Fuels 21 (2007) 1792–1815.
[14] A.J. Foster, P.T.M. Do, R.F. Lobo, Top. Catal. 55 (2012) 118–128.
[15] C. Zhao, Y. Kou, A.A. Lemonidou, X.B. Li, J.A. Lercher, Chem. Commun. 46 (2010) 412–414.
[16] X. Zhu, L.L. Lobban, R.G. Mallinson, D.E. Resasco, J. Catal. 281 (2011) 21–29.
[17] J.H. Sinfelt, Catal. Today 29 (1973) 308.
[18] R. Olcese, M.M. Bettahar, D. Petijean, B. Malaman, F. Giovanella, A. Dufour, Appl. Catal. B 115–116 (2012) 63–73.
[19] A. Ausavasukhi, T. Sooknoi, D.E. Resasco, J. Catal. 268 (2009) 68–78.
[20] A. Ausavasukhi1, Y. Huang, A.T. To, T. Sooknoi, D.E. Resasco, J. Catal. 290 (2012) 90–100.
[21] A. Cho, J. Shin, A. Takagaki, R. Kikuchi, T.S. Oyama, Top. Catal. 55 (2012) 969–980.
[22] C. Zhao, S. Kasakov, J. He, J.A. Lercher, J. Catal. 296 (2012) 12–23.
[23] X. Zhang, T. Wang, L. Ma, Q. Zhang, Y. Yu, Q. Liu, Catal. Commun. 33 (2013) 15–19.
[24] M.V. Bykova, D.Y. Ermakov, V.V. Kaichev, O.A. Bulavchenko, A.A. Saraev, M.Y. Lebedev, V.A. Yakovlev, Appl. Catal. B 113–114 (2012) 296–307.
[25] V.A. Yakovlev, S.A. Khromova, O.V. Sherstyuk, V.O. Dundich, D.Y. Ermakov, V.M. Novopashina, M.Y. Lebedev, O. Bulavchenko, V.N. Parmon, Catal. Today 144 (2009) 362–366.
[26] S. Sitthisa, W. An, D.E. Resasco, J. Catal. 284 (2011) 90–101.
[27] M. Badawi, J.-F. Paul, E. Payen, Y. Romero, F. Richard, S. Brunet, A. Popov, E. Kondratieva, J.-P. Gilson, L. Mariey, A. Travert, F. Maugé, Oil Gas Sci. Technol. (2013), http://dx.doi.org/10.2516/ogst/2012041.
[28] E.O. Odebunmi, D.F. Ollis, J. Catal. 80 (1983) 56–64.
[29] G. Kresse, J. Hafner, Phys. Rev. B 48 (17) (1993) 13115–13118.
[30] G. Kresse, J. Furthmuller, Phys. Rev. B 54 (16) (1996) 11169–11186.
[31] J.P. Perdew, K. Burke, Phys. Rev. Lett. 77 (18) (1996) 3865–3868.
[32] P.E. Blochl, Phys. Rev. B 50 (24) (1994) 17953–17979.
[33] G. Kresse, D. Joubert, Phys. Rev. B 59 (3) (1999) 1758–1775.
[34] A.V. Ruban, H.L. Skriver, J.K. Norskov, Phys. Rev. B 59 (24) (1999) 15990–16000.
[35] G.B. Raupp, W.N. Delgass, J. Catal. 58 (3) (1979) 337–347.
[36] L. Wang, D. Li, M. Koik, S. Koso, Y. Nakagawa, Y. Xu, K. Tomishige, Appl. Catal. A 392 (2011) 248–255.
[37] A.P. Legrand, H. Hommel, A. Tuel, A. Vidal, H. Balard, E. Papirer, P. Levitz, M. Czernichowski, R. Erre, H. Van Damme, J.P. Gallas, J.F. Hemidy, J.C. Lavalley, O. Barres, A. Burneau, Y. Grillet, Adv. Colloid Interface Sci. 33 (1990) 91.
[38] H.E. Bergna, W.O. Roberts, Surfactant Science Series, vol. 131, 2006.
[39] L. Oliviero, A. Vimont, J.-C. Lavalley, F.R. Sarria, M. Gaillard, F. Mauge, Phys. Chem. Chem. Phys. 7 (2005) 1861–1869.
[40] G. Connell, A. Dumesic, J. Catal. 105 (1987) 285–298.
[41] K. Hadjiivanov, M. Mihaylov, D. Klissurski, P. Stefanov, N. Abadjieva, E. Vassileva, L. Mintchevz, J. Catal. 185 (1999) 314–323.
[42] P.N. Rylander, Catalytic Hydrogenation Over Platinum Metals, Academic Press, New York, 1967, pp. 309.
[43] G.C. Bond, Platinum Metals Rev. 12 (3) (1968) 100–105.
[44] M.L. Honkela, J. Bjork, M. Persson, Phys. Chem. Chem. Phys. 14 (2012) 5849–5854.
[45] L. Delle Site, A. Alavi, C.F. Abrams, Phys. Rev. B 67 (2003) 193406.
[46] M.L. Honkela, J. Bjork, M. Perssonbd, Phys. Chem. Chem. Phys. 14 (2012) 5849–5854.
[47] S.D. Lin, M.A. Vannice, J. Catal. 143 (1993) 554–562.
[48] J. Beccat, J.C. Bertolini, Y. Gauthier, J. Massardier, P. Ruiz, J. Catal. 126 (1990) 451.
[49] T. Birchem, C.M. Pradier, Y. Berthier, G. Cordier, J. Catal. 161 (1996) 68.
[50] A. Borgna, B.G. Anderson, A.M. Saib, H. Bluhm, M. Havecker, A. Knop-Gericke, A.E.T. Kuiper, Y. Tamminga, J.W.J. Niemantsverdriet, Phys. Chem. B 108 (2004) 17905.
[51] T.B.L.W. Marinelli, S. Naubuurs, V. Ponec, J. Catal. 151 (1995) 431.
[52] T.B.L.W. Marinelli, V. Ponec, J. Catal. 156 (1995) 51.
[53] E. Shin, M.A. Keane, Ind. Eng. Chem. Res. 39 (2000) 883–892.
[54] G.V. Smith, F. Notheisz, Heterogeneous Catalysis in Organic Chemistry, Academic Press, 1999.
[55] K.J. Yoon, M.A. Vannice, J. Catal. 82 (1983) 457–468.